



HAL
open science

Heavy Quarkonium Production in Z Decays

M. Acciarri, P. Achard, O. Adriani, M. Aguilar-Benitez, J. Alcaraz, G. Alemanni, J. Allaby, A. Aloisio, M G. Alviggi, G. Ambrosi, et al.

► **To cite this version:**

M. Acciarri, P. Achard, O. Adriani, M. Aguilar-Benitez, J. Alcaraz, et al.. Heavy Quarkonium Production in Z Decays. *Physics Letters B*, 1999, 453, pp.94-106. 10.1016/S0370-2693(99)00280-4 . in2p3-00003490

HAL Id: in2p3-00003490

<https://hal.in2p3.fr/in2p3-00003490>

Submitted on 18 May 1999

HAL is a multi-disciplinary open access archive for the deposit and dissemination of scientific research documents, whether they are published or not. The documents may come from teaching and research institutions in France or abroad, or from public or private research centers.

L'archive ouverte pluridisciplinaire **HAL**, est destinée au dépôt et à la diffusion de documents scientifiques de niveau recherche, publiés ou non, émanant des établissements d'enseignement et de recherche français ou étrangers, des laboratoires publics ou privés.

Heavy Quarkonium Production in Z Decays

The L3 Collaboration

Abstract

We report measurements of the inclusive production of heavy quarkonium states in Z decays based on the analysis of 3.6 million hadronic events collected by the L3 detector at LEP. The measurement of inclusive J production and an improved 95% confidence level upper limit on Υ production are presented. In addition, two independent measurements of the ratio, f_p , of prompt J mesons to those from B decay are made using two different isolation cuts to separate prompt J mesons from J mesons produced in the decays of b hadrons. The results are:

$$\begin{aligned} \text{Br}(Z \rightarrow J + X) &= (3.21 \pm 0.21 \text{ (stat.) } {}^{+0.19}_{-0.28} \text{ (sys.)}) \times 10^{-3} , \\ \text{Br}(Z \rightarrow \Upsilon(1S) + X) &< 4.4 \times 10^{-5} , \\ f_p &= (7.1 \pm 2.1 \text{ (stat.) } \pm 1.2 \text{ (sys.) } {}^{+1.5}_{-0.8} \text{ (theo.)}) \times 10^{-2} . \end{aligned}$$

Submitted to *Phys. Lett. B*

Introduction

B-hadron decays are responsible for the majority of J mesons observed in e^+e^- collisions at the Z pole. However, heavy quarkonium production theory suggests that between 2.5% and 8.5% of all J mesons are produced via QCD mechanisms [1–3]. The older version of the theory based on the Colour Singlet Model (CSM), in which only $c\bar{c}$ pairs initially in a colour singlet state can bind to form a J, yields the lower value in this range for the prompt J fraction [1–6]. A more recent version, utilizing a nonrelativistic QCD (NRQCD) factorization formalism that involves contributions from colour octet states as well, predicts values roughly three times higher [7,8].

Upsilon states can only be produced by various QCD mechanisms because there is no analogous t-hadron decay process. Consequently, Υ states are much less common than their charmonium counterparts.

Interest in the study of prompt J and Υ mesons is motivated by the experimental excess of heavy quarkonium states in $p\bar{p}$ collisions at high p_t observed by the CDF Collaboration [9,10]. In order to explain the overabundance of such states, theoreticians have proposed a number of extensions to the previously accepted CSM, including feed-down from as yet undiscovered higher radial and angular momentum $Q\bar{Q}$ bound states, fragmentation, and colour octet contributions [11–17]. The most likely explanation for the excess of heavy quarkonium states at CDF is the participation of colour octet states in the process of gluon fragmentation [18–23]. Recently it has been pointed out that LEP results are particularly favourable to determine the octet matrix elements [24].

Three QCD mechanisms have been investigated theoretically for their roles in prompt J and Υ production at LEP. These are heavy quark fragmentation, gluon fragmentation, and gluon radiation (see Figure 1). Calculations of the colour singlet and colour octet contributions to prompt J production from the gluon radiation process are shown in Table 1. If only colour singlet processes are taken into account, the theoretical inclusive branching ratio to prompt J mesons is $\text{Br}(Z \rightarrow J_{\text{prompt}} + X) = 9.1 \times 10^{-5}$. On the other hand, if the colour octet processes are included in the prompt J production estimates, the resulting branching ratio is $\text{Br}(Z \rightarrow J_{\text{prompt}} + X) = 2.8 \times 10^{-4}$.

The rates for Υ production follow this same general pattern, although the colour singlet gluon fragmentation process is less important, and neither the colour singlet nor colour octet gluon radiation processes are as suppressed as they are for prompt J production [25,26]. For colour singlet processes, Υ production is strongly dominated by the b-fragmentation mechanism, and the branching ratio of the Z to Υ states is roughly $\text{Br}(Z \rightarrow \Upsilon + X) = 1.7 \times 10^{-5}$. Inclusion of the colour octet gluon fragmentation contribution yields a significantly larger estimate of $\text{Br}(Z \rightarrow \Upsilon + X) = 5.9 \times 10^{-5}$.

Total J Production

The present analysis is performed on the data collected by the L3 experiment [27] from 1991 through 1995 corresponding to 3.592×10^6 hadronic Z decays. After passing the data through a hadronic pre-selection, J mesons are selected using the decays $J \rightarrow \mu^+\mu^-$ and $J \rightarrow e^+e^-$, which together account for 12% of all J decays [28]. J candidates are identified by the presence of a $\mu^+\mu^-$ or e^+e^- pair with an opening angle smaller than 90° . The L3 lepton selection criteria are employed to guarantee rejection of hadronic particles. Electrons are identified by the energy deposition in the electromagnetic calorimeter which must be consistent with the expected shower shape. Furthermore, good p_t and ϕ matching between the electron clusters and

their associated tracks are required. For muons, the reconstructed tracks must pass through at least two of the three muon chamber layers and have an origin consistent with the interaction point. Minimum momentum cuts are also applied in order to improve the lepton signal-to-background ratio. This general J selection has been tested with JETSET 7.4 [29] Monte Carlo samples of 30000 events each of the type $b \rightarrow J \rightarrow \mu^+\mu^-$ and $b \rightarrow J \rightarrow e^+e^-$. The response of the L3 detector was modelled with the GEANT detector simulation program [30]. Efficiencies have been determined taking into account corrections due to time-dependent effects yielding $\epsilon_{J \rightarrow \mu^+\mu^-} = 31.3\%$ and $\epsilon_{J \rightarrow e^+e^-} = 24.7\%$.

Applying the general J selection to the data, the invariant mass distributions in Figure 2 are obtained. Clear peaks are observed in both the $\mu^+\mu^-$ and e^+e^- channels near the J mass, and smaller excesses are seen near the ψ' mass. In order to determine the number of J mesons collected, each distribution is fit (binned fit) with a third-order polynomial for the background and a two Gaussian with different widths for each vector meson peak. Studies of the Monte Carlo J and ψ' lineshapes are used to constrain some of the parameters of the Gaussian in order to reduce the total number of degrees of freedom in the fit. The number of J mesons in each decay channel is found from the integral of the individual lineshapes measured in the data. An independent determination is made by subtracting from the data distributions the properly normalised backgrounds from Monte Carlo $q\bar{q}$ events, fitting the difference with a Gaussian, and correcting the integral of this Gaussian by factors determined from the Monte Carlo lineshapes. Averaging these consistent measurements yields $N_{J \rightarrow \mu^+\mu^-} = 288 \pm 29$ and $N_{J \rightarrow e^+e^-} = 265 \pm 23$ where the error is statistical only. Using these measured numbers of J mesons, the selection efficiencies, $\text{Br}(Z \rightarrow q\bar{q}) = 0.699 \pm 0.0015$, and $\text{Br}(J \rightarrow \ell^+\ell^-) = 0.0601 \pm 0.0019$ [28], we obtain:

$$\begin{aligned} \text{Br}(Z \rightarrow J + X)_{e^+e^-} &= (3.45 \pm 0.30 \text{ (stat.) } \begin{matrix} +0.31 \\ -0.46 \end{matrix} \text{ (sys.)}) \times 10^{-3} , \\ \text{Br}(Z \rightarrow J + X)_{\mu^+\mu^-} &= (2.96 \pm 0.30 \text{ (stat.) } \begin{matrix} +0.23 \\ -0.34 \end{matrix} \text{ (sys.)}) \times 10^{-3} . \end{aligned}$$

A full description of the systematic error is provided in Table 2. Combining these values gives the final L3 measurement of the total inclusive J production in Z decays:

$$\text{Br}(Z \rightarrow J + X) = (3.21 \pm 0.21 \text{ (stat.) } \begin{matrix} +0.19 \\ -0.28 \end{matrix} \text{ (sys.)}) \times 10^{-3} .$$

This is in good agreement with our previously published value [31].

Prompt J Production

The main difficulty in measuring the prompt J production in Z decays is separating it from the much more abundant number of J's from B decay. In order to study the properties of prompt J mesons in Z decays, samples of 10000 simulated events are produced for each of the four most important QCD production processes (Table 1) using a dedicated heavy quarkonium Monte Carlo generator developed by the OPAL Collaboration [32]. Two independent analyses are performed on the full L3 Z data set, yielding two measurements (A and B) of the quantity $f_p = N_{J\text{-prompt}}/N_{J\text{-b-hadron}}$. For each of these measurements, two different J selections are used: a very general J selection (selection 1) and a prompt J selection (selection 2) with powerful rejection of J's from b-hadron decay. The general J selection used for measurement A is the same as that described in the previous section for the measurement of the total J production. For measurement B the general J selection cuts used in a previous publication [31] are applied. The efficiencies for both measurements, combined for the $\mu^+\mu^-$ and the e^+e^- final states are shown in Table 3.

For the first measurement (A) of f_p , a selection of prompt J mesons is based on the isolation energy parameter E_{30} . This variable is defined as the energy measured within a 30° cone of the candidate J direction, excluding the energy of the J candidate itself. Distributions of E_{30} for prompt J mesons produced via different QCD mechanisms with respect to J mesons originating from b-hadron decays are shown in Figure 3. A modest separation is observed for colour singlet c-fragmentation J's, and nearly complete separation is observed for colour octet gluon-fragmentation J's. Guided by these distributions, the following cuts are applied:

- $E_{30-ee} < 2.5 \text{ GeV}$, $E_{30-\mu\mu} < 4.0 \text{ GeV}$.

Different cuts are used for $J \rightarrow e^+e^-$ and $J \rightarrow \mu^+\mu^-$ candidates because E_{30} must be calculated differently for the electron and muon J decay modes. The efficiencies which are obtained with this selection are reported in the first column of Table 4. The $\mu^+\mu^-$ and the e^+e^- final states have been combined.

For the second measurement (B) of f_p , the angle between the J candidate direction and the nearest jet axis, $\alpha_{J\text{-jet}}$, is used to suppress the background of J's stemming from b-hadron decay. From the distributions of this variable in Figure 4, it is clear that cuts on $\alpha_{J\text{-jet}}$ can be especially effective in selecting J mesons from gluon fragmentation, which are often quite isolated. Based on this information, the following cut is used for the second selection of prompt J mesons:

- $\alpha_{J\text{-jet}} > 40^\circ$.

The remainder of the cuts are the same as for the general J selection used in a previous publication [31]. The resulting efficiencies from this selection are reported in the second column of Table 4. The $\mu^+\mu^-$ and the e^+e^- final states have been combined.

Applying the prompt selection of measurement A to the data, the invariant mass distribution shown in Figure 5a is obtained. Here, the $J \rightarrow e^+e^-$ and $J \rightarrow \mu^+\mu^-$ results have been combined. Two independent methods are employed to estimate the background in the signal region from 2.733 GeV to 3.467 GeV. The first method is to fit the data invariant mass distribution using a third-order polynomial for the background and a Gaussian for the J peak. The result of the fit is that of the 53 events in the J region 28 ± 6.4 are attributed to the J signal with a background of 25 events. In the second method the background is estimated by using a large sample of Monte Carlo $q\bar{q}$ events and rescaling. This yields 25 ± 6.4 events for the J signal and 28 for the background. Combining the two methods of estimating the background one obtains for measurement A 27.5 ± 6.5 events for the J signal with a systematic error of about 2.8 events due to the fitting procedure.

A similar analysis of the data selected with the measurement B prompt selection has been performed. The invariant mass distribution which is obtained when combining the $J \rightarrow e^+e^-$ and $J \rightarrow \mu^+\mu^-$ channels is shown in Figure 5b. Two methods were used to estimate the background of the 29 events found in the invariant mass region from 2.8 GeV to 3.4 GeV. First the data were fit in the range from 1.8 GeV to 5.5 GeV using two straight lines (joint quadratically) and a Gaussian for the J peak, giving a J signal of 17.1 events and a background of 11.9 events. The second estimate is obtained by applying the cuts to the Monte Carlo hadronic sample and scaling it which gives 11.4 events. Combining the two estimates a J signal of 17.4 events with a background of 11.6 events and a systematic error of about 0.5 events is obtained for measurement B. Without isolation cut the sum of J mesons from both the electron and muon channel is 392.

Using these numbers of J mesons and the efficiencies in Tables 3 and 4, two separate measurements of f_p are made using:

$$f_p = \frac{N_2 \cdot \epsilon_b^1 - N_1 \cdot \epsilon_b^2}{N_1 \cdot \epsilon_p^2 - N_2 \cdot \epsilon_p^1}, \quad (1)$$

where N_1 and N_2 are the number of measured J candidates for selections 1 and 2, respectively. Including the systematic errors summarised in Table 5, the results are:

$$\text{Measurement A: } f_p = (7.0 \pm 2.3 \text{ (stat.)} \pm 1.4 \text{ (sys.)} \pm_{-0.6}^{+1.0} \text{ (theo.)}) \times 10^{-2} ;$$

$$\text{Measurement B: } f_p = (7.7 \pm 3.3 \text{ (stat.)} \pm 1.0 \text{ (sys.)} \pm_{-0.9}^{+1.7} \text{ (theo.)}) \times 10^{-2} .$$

The systematic errors are shown in Table 5. The theoretical errors were estimated by changing the theoretical branching ratios of Table 1 by factors of 2 in both directions. The values of f_p imply that for measurement A of the 27.5 events in the J signal 21.2 originate from prompt production and 6.3 from B decay. The corresponding numbers for measurement B are 12.3 prompt J and 5.1 from B decay of the total of 17.4.

It should be noted that there is an advantage in expressing the prompt J production in terms of a ratio to the production of J mesons from b-hadron decays. By doing this, the systematic errors common to the measurements of $\text{Br}(Z \rightarrow J_{\text{b-hadron}} + X) \approx \text{Br}(Z \rightarrow J + X)$ and $\text{Br}(Z \rightarrow J_{\text{prompt}} + X)$ cancel, including the errors on $\text{Br}(J \rightarrow \ell^+ \ell^-)$ and $\text{Br}(Z \rightarrow q\bar{q})$, and most of the error involved with the J selection. Combining the two measurements above, taking into account the correlated statistical errors (correlation is about 50%), yields:

$$f_p = (7.1 \pm 2.1 \text{ (stat.)} \pm 1.2 \text{ (sys.)} \pm_{-0.8}^{+1.5} \text{ (theo.)}) \times 10^{-2} .$$

This value of f_p is then converted into a measurement of the inclusive branching ratio of the Z to prompt J mesons by using the measured value of $\text{Br}(Z \rightarrow J + X)$ obtained in the last section and taking into account that $f_p = N_{J\text{-prompt}}/N_{J\text{-b-hadron}} \neq N_{J\text{-prompt}}/N_{J\text{-total}}$. This calculation gives:

$$\text{Br}(Z \rightarrow J_{\text{prompt}} + X) = (2.1 \pm 0.6 \text{ (stat.)} \pm 0.4 \text{ (sys.)} \pm_{-0.2}^{+0.4} \text{ (theo.)}) \times 10^{-4} .$$

For the purpose of comparison, the theoretical branching ratio obtained by combining the colour singlet and colour octet predictions in Table 1 is 2.8×10^{-4} whereas it is only 0.9×10^{-4} for singlet contributions. Thus, the data prefer the inclusion of color octet processes.

Upsilon Production

To study the Υ signal and estimate the selection efficiencies, samples of 10000 events for each of the Υ QCD production processes are generated using the same Monte Carlo used for the production of the prompt J samples [32]. Upsilon mesons are identified by the dileptonic decay modes $\Upsilon \rightarrow \mu^+ \mu^-$ and $\Upsilon \rightarrow e^+ e^-$, which together represent 5% of all Υ decays [28]. The selection procedure follows that for prompt J mesons closely, starting with a standard hadronic pre-selection and the subsequent search for $\mu^+ \mu^-$ or $e^+ e^-$ pairs. Similar cuts are imposed on lepton candidates. In the case of $\Upsilon \rightarrow e^+ e^-$ candidates, both of the electrons must have momentum greater than 4 GeV, and for $\Upsilon \rightarrow \mu^+ \mu^-$ candidates, the muon momenta must be larger than 2 GeV.

The isolation cuts for the detection of prompt Υ mesons can be much looser than for prompt J since there are no Υ from t decay. The isolation cut is used only to suppress background from spurious $\mu^+\mu^-$ and e^+e^- combinations events where the leptons originate, for instance, from two different D or B decays. For the Υ case, MC studies showed that the angle between the most energetic lepton and the nearest jet, $\alpha_{\text{lep1-jet}}$, is the most favourable variable to suppress background (see Figure 6).

To detect Υ 's from the first four processes in Table 1, the following cuts were applied: $\alpha_{\text{lep1-jet}} > 13^\circ$ and $\alpha_{\text{lep2-jet}} > 3^\circ$ for $\mu^+\mu^-$ events and $\alpha_{\text{lep1-jet}} > 6.75^\circ$ for e^+e^- events, where $\alpha_{\text{lep2-jet}}$ is the angle between the second most energetic lepton and the nearest jet.

The fifth process in Table 1 is essentially a two-body decay of the Z and is more easily identified. For events in which the most energetic lepton and the nearest jet are in opposite hemispheres, the angle cuts $\alpha_{\text{lep1-jet}} > 150^\circ$ for $\mu^+\mu^-$ and $\alpha_{\text{lep1-jet}} > 90^\circ$ for e^+e^- events are chosen. However, for this process some of the events have $\alpha_{\text{lep1-jet}}$ angles close to zero, and for these cases the following cuts are used: the energy of the nearest jet > 8 GeV for $\mu^+\mu^-$ events and $\alpha_{\text{lep1-jet}} < 15^\circ$ for e^+e^- events.

Processing all the Z decay events in the L3 data set through the Υ selection just described yields the invariant mass distributions shown in Figure 7. Examination of these distributions reveals that the background is low in the invariant mass range from 7 GeV to 9 GeV and is in agreement with the Monte Carlo expectation not shown in the Figure. In calculating the limits also the background of 4-fermion events was taken into account. There is only one signal candidate in the e^+e^- channel in the peak regions of the Υ states which is consistent with the background expectations. In the absence of a signal, upper limits at the 95% confidence level (CL) on the branching ratios $\text{Br}(Z \rightarrow \Upsilon(1S) + X)$ for each of the Υ production mechanisms are established from binned maximum-likelihood fits to the $\ell^+\ell^-$ invariant mass distributions, following the same method outlined in [33]. The results are given in Table 6. In calculating the 95% CL limits, various systematic errors are taken into account, the most important being the uncertainty in $\text{Br}(\Upsilon \rightarrow \ell^+\ell^-)$ (2.6%) and the uncertainty in the Υ polarisation (6%) [33]. The weighted sum takes into account the various theoretical branching ratios.

Conclusions

Using our complete sample of hadronic Z decays we obtain for the inclusive J branching ratio:

$$\text{Br}(Z \rightarrow J + X) = (3.21 \pm 0.21 \text{ (stat.) } {}_{-0.28}^{+0.19} \text{ (sys.)}) \times 10^{-3} .$$

This value is in good agreement with other measurements made at LEP [34–36]. This analysis also shows that prompt J mesons produced by various QCD mechanisms are present in measurable quantities, allowing for the determination of f_p and $\text{Br}(Z \rightarrow J_{\text{prompt}} + X)$:

$$\begin{aligned} f_p &= (7.1 \pm 2.1 \text{ (stat.) } \pm 1.2 \text{ (sys.) } {}_{-0.8}^{+1.5} \text{ (theo.)}) \times 10^{-2} , \\ \text{Br}(Z \rightarrow J_{\text{prompt}} + X) &= (2.1 \pm 0.6 \text{ (stat.) } \pm 0.4 \text{ (sys.) } {}_{-0.2}^{+0.4} \text{ (theo.)}) \times 10^{-4} . \end{aligned}$$

The positive observation of prompt J mesons is in accord with the findings of a similar study of prompt J production performed recently [37]. In addition, the measured value of $\text{Br}(Z \rightarrow J_{\text{prompt}} + X)$ is in good agreement with recent theoretical calculations of prompt J production in Z decays, which include both colour singlet and colour octet contributions. However, the measured $\text{Br}(Z \rightarrow J_{\text{prompt}} + X)$ disagrees with the leading order Colour Singlet Model prediction at the two standard deviation level. Such disagreement is also observed for

χ_{c1} production at L3 [31]. This evidence suggests that the CSM might not provide an adequate description of heavy quarkonia production in e^+e^- collisions at the Z pole and lends support to the hypothesis that other mechanisms such as colour octet gluon fragmentation are involved.

We have also searched for Υ production in Z decays and have obtained the following 95% confidence level upper limit:

$$\text{Br}(Z \rightarrow \Upsilon(1S) + X) < 4.4 \times 10^{-5}$$

This limit is in agreement with the theoretical prediction, taking into account colour octet contributions. It improves upon previously published limits [33, 38] and may be compared to the measured value in [39].

Acknowledgements

We wish to thank the OPAL Collaboration for the use of its dedicated heavy quarkonium Monte Carlo in generating the Monte Carlo samples required for this analysis. In addition, we wish to express our gratitude to the CERN accelerator divisions for the excellent performance of the LEP machine. We acknowledge the contributions of all the engineers and technicians who have participated in the construction and maintenance of this experiment.

References

- [1] K. Hagiwara, A.D. Martin, and W.J. Stirling, Phys. Lett. **B 267** (1991) 527; Erratum ibid. **B 316** (1993) 631.
- [2] E. Braaten and T.C. Yuan, Phys. Rev. Lett. **71** (1993) 1673.
- [3] W.-Y. Keung, Phys. Rev. **D 23** (1981) 2072.
- [4] V. Barger, K. Cheung and W.-Y. Keung, Phys. Rev. **D 41** (1990) 1541.
- [5] E. Braaten, K. Cheung and T.C. Yuan, Phys. Rev. **D 48** (1993) 4230.
- [6] E.J. Eichten and C. Quigg, Phys. Rev. **D 52** (1995) 1726.
- [7] P. Cho, Phys. Lett. **B 368** (1996) 171.
- [8] K. Cheung, W.-Y. Keung, and T.C. Yuan, Phys. Rev. Lett. **76** (1996) 877.
- [9] CDF Collaboration, F. Abe *et al.*, Phys. Rev. Lett. **69** (1992) 3704.
- [10] CDF Collaboration, F. Abe *et al.*, Phys. Rev. Lett. **75** (1995) 4358.
- [11] P. Cho *et al.*, Phys. Rev. **D 51** (1995) 2039.
- [12] P. Cho and M.B. Wise, Phys. Lett. **B 346** (1995) 129.
- [13] F.E. Close, Phys. Lett. **B 342** (1995) 369.
- [14] D.P. Roy and K. Sridhar, Phys. Lett. **B 345** (1995) 537.
- [15] M. Cacciari and M. Greco, Phys. Rev. Lett. **73** (1994) 1586.
- [16] M. Cacciari, M. Greco, M.L. Mangano and A. Petrelli, Phys. Lett. **B 356** (1995) 553.
- [17] D.P. Roy and K. Sridhar, Phys. Lett. **B 339** (1994) 141.
- [18] G.T. Bodwin, E. Braaten and G.P. Lepage, Phys. Rev. **D 51** (1995) 1125; Erratum ibid **D 55** (1997) 5853.
- [19] E. Braaten and Y. Chen, Phys. Rev. Lett. **76** (1996) 1417.
- [20] P. Ko, J. Lee and H.S. Song, Phys. Rev. **D 54** (1996) 4312.
- [21] M. Beneke and M. Kraemer, Phys. Rev. **D 55** (1997) 5269.
- [22] P. Cho and A.K. Leibovich, Phys. Rev. **D 53** (1996) 150.
- [23] P. Cho and A.K. Leibovich, Phys. Rev. **D 53** (1996) 6203.
- [24] C.G. Boyd, A.K. Leibovich and I.Z. Rothstein, Carnegie Mellon Univ., CMU-HEP 98-03.
- [25] K.J. Abraham, Z. Phys. **C 44** (1989) 467.
- [26] J.H.Kuhn and H.Schneider, Z. Phys. **C11** (1981) 263.

- [27] L3 Collaboration, B. Adeva *et al.*, Nucl. Inst. Meth. **A 289** (1990) 35;
O. Adriani *et al.*, Nucl. Inst. Meth. **A302** (1991) 53;
K. Deiters *et al.*, Nucl. Inst. Meth. **A323** (1992) 162;
M. Acciari *et al.*, Nucl. Inst. Meth. **A 351** (1994) 300.
- [28] Particle Data Group, R.M. Barnett *et al.*, Phys. Rev. **D 54** (1996) 1.
- [29] T. Sjöstrand, Comp. Phys. Comm. **39** (1986) 347;
T. Sjöstrand and M. Bengtsson, Comp. Phys. Comm. **43** (1987) 367.
- [30] The L3 detector simulation is based on GEANT Version 3.15.
R. Brun *et al.*, *GEANT 3*, CERN-DD/EE/84-1 (Revised), 1987.
The GHEISHA program (H. Fesefeldt, RWTH Aachen Report PITHA 85/02 (1985))
is used to simulate hadronic interactions.
- [31] L3 Collaboration, M. Acciarri *et al.*, Phys. Lett. **B 407** (1997) 351.
- [32] OPAL Collaboration, private communication.
- [33] L3 Collaboration, M. Acciari *et al.*, Phys. Lett. **B 413** (1997) 167.
- [34] ALEPH Collaboration, D. Buskulic *et al.*, Phys. Lett. **B 295** (1992) 396.
- [35] DELPHI Collaboration, P. Abreu, *et al.*, Phys. Lett. **B 341** (1994) 109.
- [36] OPAL Collaboration, G. Alexander *et al.*, Z. Phys. **C 70** (1996) 197.
- [37] OPAL Collaboration, G. Alexander *et al.*, Phys. Lett. **B 384** (1996) 343.
- [38] DELPHI Collaboration, P. Abreu, *et al.*, Z. Phys. **C 69** (1996) 575.
- [39] OPAL Collaboration, G. Alexander *et al.*, Phys. Lett. **B 370** (1996) 185.

The L3 Collaboration:

M. Acciarri,²⁶ P. Achard,¹⁸ O. Adriani,¹⁵ M. Aguilar-Benitez,²⁵ J. Alcaraz,²⁵ G. Alemanni,²¹ J. Allaby,¹⁶ A. Aloisio,²⁸ M.G. Alvigi,²⁸ G. Ambrosi,¹⁸ H. Anderhub,⁴⁷ V.P. Andreev,^{6,36} T. Angelescu,¹² F. Anselmo,⁹ A. Arefiev,²⁷ T. Azemoon,³ T. Aziz,¹⁰ P. Bagnaia,³⁵ L. Baksay,⁴² A. Balandras,⁴ R.C. Ball,³ S. Banerjee,¹⁰ Sw. Banerjee,¹⁰ K. Banicz,⁴⁴ A. Barczyk,^{47,45} R. Barillere,¹⁶ L. Barone,³⁵ P. Bartalini,²¹ M. Basile,⁹ R. Battiston,³² A. Bay,²¹ F. Becattini,¹⁵ U. Becker,¹⁴ F. Behner,⁴⁷ J. Berdugo,²⁵ P. Berges,¹⁴ B. Bertucci,³² B.L. Betev,⁴⁷ S. Bhattacharya,¹⁰ M. Biasini,³² A. Biland,⁴⁷ J.J. Blaising,⁴ S.C. Blyth,³³ G.J. Bobbink,² A. Böhm,¹ L. Boldizsar,¹³ B. Borgia,^{16,35} D. Bourilkov,⁴⁷ M. Bourquin,¹⁸ S. Braccini,¹⁸ J.G. Branson,³⁸ V. Brigljevic,⁴⁷ F. Brochu,⁴ A. Buffini,¹⁵ A. Buijs,⁴³ J.D. Burger,¹⁴ W.J. Burger,³² J. Busenitz,⁴² A. Button,³ X.D. Cai,¹⁴ M. Campanelli,⁴⁷ M. Capell,¹⁴ G. Cara Romeo,⁹ G. Carlino,²⁸ A.M. Cartacci,¹⁵ J. Casaus,²⁵ G. Castellini,¹⁵ F. Cavallari,³⁵ N. Cavallo,²⁸ C. Cecchi,¹⁸ M. Cerrada,²⁵ F. Cesaroni,²² M. Chamizo,²⁵ Y.H. Chang,⁴⁹ U.K. Chaturvedi,¹⁷ M. Chemarin,²⁴ A. Chen,⁴⁹ G. Chen,⁷ G.M. Chen,⁷ H.F. Chen,¹⁹ H.S. Chen,⁷ X. Chereau,⁴ G. Chiefari,²⁸ L. Cifarelli,³⁷ F. Cindolo,⁹ C. Civinini,¹⁵ I. Clare,¹⁴ R. Clare,¹⁴ G. Coignet,⁴ A.P. Colijn,² N. Colino,²⁵ S. Costantini,⁸ F. Cotorobai,¹² B. de la Cruz,²⁵ A. Csilling,¹³ T.S. Dai,¹⁴ J.A. van Dalen,³⁰ R. D'Alessandro,¹⁵ R. de Asmundis,²⁸ P. Deglon,¹⁸ A. Degré,⁴ K. Deiters,⁴⁵ D. della Volpe,²⁸ P. Denes,³⁴ F. DeNotaristefani,³⁵ A. De Salvo,⁴⁷ M. Diemoz,³⁵ D. van Dierendonck,² F. Di Lodovico,⁴⁷ C. Dionisi,^{16,35} M. Dittmar,⁴⁷ A. Dominguez,³⁸ A. Doria,²⁸ M.T. Dova,^{17,4} D. Duchesneau,⁴ D. Dufournand,⁴ P. Duinker,² I. Duran,³⁹ H. El Mamouni,²⁴ A. Engler,³³ F.J. Eppling,¹⁴ F.C. Erné,² P. Extermann,¹⁸ M. Fabre,⁴⁵ R. Faccini,³⁵ M.A. Falagan,²⁵ S. Falciano,³⁵ A. Favara,¹⁵ J. Fay,²⁴ O. Fedin,³⁶ M. Felcini,⁴⁷ T. Ferguson,³³ F. Ferroni,³⁵ H. Fesefeldt,¹ E. Fiandrini,³² J.H. Field,¹⁸ F. Filthaut,¹⁶ P.H. Fisher,¹⁴ I. Fisk,³⁸ G. Forconi,¹⁴ L. Fredj,¹⁸ K. Freudenreich,⁴⁷ C. Furetta,²⁶ Yu. Galaktionov,^{27,14} S.N. Ganguli,¹⁰ P. Garcia-Abia,⁵ M. Gataullin,³¹ S.S. Gau,¹¹ S. Gentile,³⁵ N. Gheordanescu,¹² S. Giagu,³⁵ S. Goldfarb,²¹ Z.F. Gong,¹⁹ M.W. Gruenewald,⁸ R. van Gulik,² V.K. Gupta,³⁴ A. Gurtu,¹⁰ L.J. Gutay,⁴⁴ D. Haas,⁵ A. Hasan,²⁹ D. Hatzifotiadou,⁹ T. Hebbeker,⁸ A. Herve,¹⁶ P. Hidas,¹³ J. Hirschfelder,³³ H. Hofer,⁴⁷ G. Holzner,⁴⁷ H. Hoorani,³³ S.R. Hou,⁴⁹ I. Iashvili,⁴⁶ B.N. Jin,⁷ L.W. Jones,³ P. de Jong,¹⁶ I. Josa-Mutuberría,²⁵ A. Kasser,²¹ R.A. Khan,¹⁷ D. Kamrad,⁴⁶ J.S. Kapustinsky,²³ M. Kaur,^{17,4} M.N. Kienzle-Focacci,¹⁸ D. Kim,³⁵ D.H. Kim,⁴¹ J.K. Kim,⁴¹ S.C. Kim,⁴¹ W.W. Kinnison,²³ J. Kirkby,¹⁶ D. Kiss,¹³ W. Kittel,³⁰ A. Klimentov,^{14,27} A.C. König,³⁰ A. Kopp,⁴⁶ I. Korolko,²⁷ V. Koutsenko,^{14,27} R.W. Kraemer,³³ W. Krenz,¹ A. Kunin,^{14,27} P. Lacentre,^{46,4,4} P. Ladron de Guevara,²⁵ I. Laktineh,²⁴ G. Landi,¹⁵ C. Lapoint,¹⁴ K. Lassila-Perini,⁴⁷ P. Laurikainen,²⁰ A. Lavorato,³⁷ M. Lebeau,¹⁶ A. Lebedev,¹⁴ P. Lebrun,²⁴ P. Lecomte,⁴⁷ P. Lecoq,¹⁶ P. Le Coultre,⁴⁷ H.J. Lee,⁸ J.M. Le Goff,¹⁶ R. Leiste,⁴⁶ E. Leonardi,³⁵ P. Levchenko,³⁶ C. Li,¹⁹ C.H. Lin,⁴⁹ W.T. Lin,⁴⁹ F.L. Linde,^{2,16} L. Lista,²⁸ Z.A. Liu,⁷ W. Lohmann,⁴⁶ E. Longo,³⁵ Y.S. Lu,⁷ K. Lübelmeyer,¹ C. Luci,^{16,35} D. Luckey,¹⁴ L. Luminari,³⁵ W. Lustermann,⁴⁷ W.G. Ma,¹⁹ M. Maity,¹⁰ G. Majumder,¹⁰ L. Malgeri,¹⁶ A. Malinin,²⁷ C. Mañá,²⁵ D. Mangeol,³⁰ P. Marchesini,⁴⁷ G. Marian,^{42,4} J.P. Martin,²⁴ F. Marzano,³⁵ G.G.G. Massaro,² K. Mazumdar,¹⁰ R.R. McNeil,⁶ S. Mele,¹⁶ L. Merola,²⁸ M. Meschini,¹⁵ W.J. Metzger,³⁰ M. von der Mey,¹ Y. Mi,²¹ D. Migani,⁹ A. Mihul,¹² H. Milcent,¹⁶ G. Mirabelli,³⁵ J. Mnich,¹⁶ P. Molnar,⁸ B. Monteleoni,¹⁵ T. Moulik,¹⁰ G.S. Muanza,²⁴ F. Muheim,¹⁸ A.J.M. Muijs,² S. Nahn,¹⁴ M. Napolitano,²⁸ F. Nessi-Tedaldi,⁴⁷ H. Newman,³¹ T. Niessen,¹ A. Nippe,²¹ A. Nisati,³⁵ H. Nowak,⁴⁶ Y.D. Oh,⁴¹ G. Organtini,³⁵ R. Ostonen,²⁰ C. Palomares,²⁵ D. Pandoulas,¹ S. Paoletti,^{35,16} P. Paolucci,²⁸ H.K. Park,³³ I.H. Park,⁴¹ G. Pascale,³⁵ G. Passaleva,¹⁶ S. Patricelli,²⁸ T. Paul,¹¹ M. Pauluzzi,³² C. Paus,¹⁶ F. Pauss,⁴⁷ D. Peach,¹⁶ M. Pedace,³⁵ Y.J. Pei,¹ S. Pensotti,²⁶ D. Perret-Gallix,⁴ B. Petersen,³⁰ S. Petrak,⁸ D. Piccolo,²⁸ M. Pieri,¹⁵ P.A. Piroué,³⁴ E. Pistolesi,²⁶ V. Plyaskin,²⁷ M. Pohl,⁴⁷ V. Pojidaev,^{27,15} H. Postema,¹⁴ J. Pothier,¹⁶ N. Produit,¹⁸ D. Prokofiev,³⁶ J. Quartieri,³⁷ G. Rahal-Callot,⁴⁷ N. Raja,¹⁰ P.G. Rancoita,²⁶ G. Raven,³⁸ P. Razis,²⁹ D. Ren,⁴⁷ M. Rescigno,³⁵ S. Reucroft,¹¹ T. van Rhee,⁴³ S. Riemann,⁴⁶ K. Riles,³ A. Robohm,⁴⁷ J. Rodin,⁴² B.P. Roe,³ L. Romero,²⁵ S. Rosier-Lees,⁴ Ph. Rosselet,²¹ J.A. Rubio,¹⁶ D. Ruschmeier,⁸ H. Rykaczewski,⁴⁷ S. Sakar,³⁵ J. Salicio,¹⁶ E. Sanchez,²⁵ M.P. Sanders,³⁰ M.E. Sarakinos,²⁰ C. Schäfer,¹ V. Schegelsky,³⁶ S. Schmidt-Kaerst,¹ D. Schmitz,¹ N. Scholz,⁴⁷ H. Schopper,⁴⁸ D.J. Schotanus,³⁰ J. Schwenke,¹ G. Schwering,¹ C. Sciacca,²⁸ D. Sciarrino,¹⁸ L. Servoli,³² S. Shevchenko,³¹ N. Shivarov,⁴⁰ V. Shoutko,²⁷ J. Shukla,²³ E. Shumilov,²⁷ A. Shvorob,³¹ T. Siedenburg,¹ D. Son,⁴¹ B. Smith,³³ P. Spillantini,¹⁵ M. Steuer,¹⁴ D.P. Stickland,³⁴ A. Stone,⁶ H. Stone,³⁴ B. Stoyanov,⁴⁰ A. Straessner,¹ K. Sudhakar,¹⁰ G. Sultanov,¹⁷ L.Z. Sun,¹⁹ H. Suter,⁴⁷ J.D. Swain,¹⁷ Z. Szillasi,^{42,4} X.W. Tang,⁷ L. Tauscher,⁵ L. Taylor,¹¹ C. Timmermans,³⁰ Samuel C.C. Ting,¹⁴ S.M. Ting,¹⁴ S.C. Tonwar,¹⁰ J. Tóth,¹³ C. Tully,³⁴ K.L. Tung,⁷ Y. Uchida,¹⁴ J. Ulbricht,⁴⁷ E. Valente,³⁵ G. Vesztegombi,¹³ I. Vetlitsky,²⁷ G. Viertel,⁴⁷ S. Villa,¹¹ M. Vivargent,⁴ S. Vlachos,⁵ H. Vogel,³³ H. Vogt,⁴⁶ I. Vorobiev,^{16,27} A.A. Vorobyov,³⁶ A. Vorvolakos,²⁹ M. Wadhwa,⁵ W. Wallraff,¹ J.C. Wang,¹⁴ X.L. Wang,¹⁹ Z.M. Wang,¹⁹ A. Weber,¹ M. Weber,¹ P. Wienemann,¹ H. Wilkens,³⁰ S.X. Wu,¹⁴ S. Wynhoff,¹ L. Xia,³¹ Z.Z. Xu,¹⁹ B.Z. Yang,¹⁹ C.G. Yang,⁷ H.J. Yang,⁷ M. Yang,⁷ J.B. Ye,¹⁹ S.C. Yeh,⁵⁰ J.M. You,³³ An. Zalite,³⁶ Yu. Zalite,³⁶ P. Zemp,⁴⁷ Z.P. Zhang,¹⁹ G.Y. Zhu,⁷ R.Y. Zhu,³¹ A. Zichichi,^{9,16,17} F. Ziegler,⁴⁶ G. Zilizi,^{42,4} M. Zöller,¹

- 1 I. Physikalisches Institut, RWTH, D-52056 Aachen, FRG[§]
 - III. Physikalisches Institut, RWTH, D-52056 Aachen, FRG[§]
 - 2 National Institute for High Energy Physics, NIKHEF, and University of Amsterdam, NL-1009 DB Amsterdam, The Netherlands
 - 3 University of Michigan, Ann Arbor, MI 48109, USA
 - 4 Laboratoire d'Annecy-le-Vieux de Physique des Particules, LAPP,IN2P3-CNRS, BP 110, F-74941 Annecy-le-Vieux CEDEX, France
 - 5 Institute of Physics, University of Basel, CH-4056 Basel, Switzerland
 - 6 Louisiana State University, Baton Rouge, LA 70803, USA
 - 7 Institute of High Energy Physics, IHEP, 100039 Beijing, China[△]
 - 8 Humboldt University, D-10099 Berlin, FRG[§]
 - 9 University of Bologna and INFN-Sezione di Bologna, I-40126 Bologna, Italy
 - 10 Tata Institute of Fundamental Research, Bombay 400 005, India
 - 11 Northeastern University, Boston, MA 02115, USA
 - 12 Institute of Atomic Physics and University of Bucharest, R-76900 Bucharest, Romania
 - 13 Central Research Institute for Physics of the Hungarian Academy of Sciences, H-1525 Budapest 114, Hungary[‡]
 - 14 Massachusetts Institute of Technology, Cambridge, MA 02139, USA
 - 15 INFN Sezione di Firenze and University of Florence, I-50125 Florence, Italy
 - 16 European Laboratory for Particle Physics, CERN, CH-1211 Geneva 23, Switzerland
 - 17 World Laboratory, FBLJA Project, CH-1211 Geneva 23, Switzerland
 - 18 University of Geneva, CH-1211 Geneva 4, Switzerland
 - 19 Chinese University of Science and Technology, USTC, Hefei, Anhui 230 029, China[△]
 - 20 SEFT, Research Institute for High Energy Physics, P.O. Box 9, SF-00014 Helsinki, Finland
 - 21 University of Lausanne, CH-1015 Lausanne, Switzerland
 - 22 INFN-Sezione di Lecce and Università Degli Studi di Lecce, I-73100 Lecce, Italy
 - 23 Los Alamos National Laboratory, Los Alamos, NM 87544, USA
 - 24 Institut de Physique Nucléaire de Lyon, IN2P3-CNRS, Université Claude Bernard, F-69622 Villeurbanne, France
 - 25 Centro de Investigaciones Energéticas, Medioambientales y Tecnológicas, CIEMAT, E-28040 Madrid, Spain^b
 - 26 INFN-Sezione di Milano, I-20133 Milan, Italy
 - 27 Institute of Theoretical and Experimental Physics, ITEP, Moscow, Russia
 - 28 INFN-Sezione di Napoli and University of Naples, I-80125 Naples, Italy
 - 29 Department of Natural Sciences, University of Cyprus, Nicosia, Cyprus
 - 30 University of Nijmegen and NIKHEF, NL-6525 ED Nijmegen, The Netherlands
 - 31 California Institute of Technology, Pasadena, CA 91125, USA
 - 32 INFN-Sezione di Perugia and Università Degli Studi di Perugia, I-06100 Perugia, Italy
 - 33 Carnegie Mellon University, Pittsburgh, PA 15213, USA
 - 34 Princeton University, Princeton, NJ 08544, USA
 - 35 INFN-Sezione di Roma and University of Rome, "La Sapienza", I-00185 Rome, Italy
 - 36 Nuclear Physics Institute, St. Petersburg, Russia
 - 37 University and INFN, Salerno, I-84100 Salerno, Italy
 - 38 University of California, San Diego, CA 92093, USA
 - 39 Dept. de Física de Partículas Elementales, Univ. de Santiago, E-15706 Santiago de Compostela, Spain
 - 40 Bulgarian Academy of Sciences, Central Lab. of Mechatronics and Instrumentation, BU-1113 Sofia, Bulgaria
 - 41 Center for High Energy Physics, Adv. Inst. of Sciences and Technology, 305-701 Taejeon, Republic of Korea
 - 42 University of Alabama, Tuscaloosa, AL 35486, USA
 - 43 Utrecht University and NIKHEF, NL-3584 CB Utrecht, The Netherlands
 - 44 Purdue University, West Lafayette, IN 47907, USA
 - 45 Paul Scherrer Institut, PSI, CH-5232 Villigen, Switzerland
 - 46 DESY-Institut für Hochenergiephysik, D-15738 Zeuthen, FRG
 - 47 Eidgenössische Technische Hochschule, ETH Zürich, CH-8093 Zürich, Switzerland
 - 48 University of Hamburg, D-22761 Hamburg, FRG
 - 49 National Central University, Chung-Li, Taiwan, China
 - 50 Department of Physics, National Tsing Hua University, Taiwan, China
- [§] Supported by the German Bundesministerium für Bildung, Wissenschaft, Forschung und Technologie
[‡] Supported by the Hungarian OTKA fund under contract numbers T019181, F023259 and T024011.
[¶] Also supported by the Hungarian OTKA fund under contract numbers T22238 and T026178.
^b Supported also by the Comisión Interministerial de Ciencia y Tecnología.
[‡] Also supported by CONICET and Universidad Nacional de La Plata, CC 67, 1900 La Plata, Argentina.
[‡] Supported by Deutscher Akademischer Austauschdienst.
[◇] Also supported by Panjab University, Chandigarh-160014, India.
[△] Supported by the National Natural Science Foundation of China.

Production Mechanism	Predicted Br($Z \rightarrow J_{\text{prompt}} + X$)		Predicted Br($Z \rightarrow \Upsilon + X$)	
singlet quark fragmentation	6.7×10^{-5}	[4–7]	1.6×10^{-5}	[4–7]
singlet gluon fragmentation	2.3×10^{-5}	[1, 2]	0.07×10^{-5}	[1, 2]
singlet gluon radiation	0.061×10^{-5}	[3, 6]	0.05×10^{-5}	[3, 25, 26]
octet gluon fragmentation	19.0×10^{-5}	[7, 22, 23]	4.1×10^{-5}	[7, 22, 23]
octet gluon radiation	0.009×10^{-5}	[7, 22, 23]	0.1×10^{-5}	[7, 22, 23]

Table 1: Theoretical predictions for the branching ratios of prompt J and Υ production in Z decays by various colour singlet and colour octet processes.

Source	$(\Delta\text{Br}/\text{Br})_{J \rightarrow e^+e^-}$ (%)	$(\Delta\text{Br}/\text{Br})_{J \rightarrow \mu^+\mu^-}$ (%)	$(\Delta\text{Br}/\text{Br})_{\text{comb.}}$ (%)
J selection	+5.4 -11.2	+3.7 -9.3	+3.3 -7.3
efficiency correction	± 6.0	± 3.5	± 3.5
Br($J \rightarrow \ell^+\ell^-$)	± 3.2	± 3.2	± 2.3
Monte Carlo statistics	± 1.5	± 1.4	± 1.0
fitting method	± 1.3	± 4.7	± 2.4
prompt J production	± 1.0	± 1.0	± 1.0
Br($Z \rightarrow q\bar{q}$)	± 0.2	± 0.2	± 0.2
Total	+9.0 -13.3	+7.8 -11.6	+6.0 -8.9

Table 2: Sources and magnitudes of systematic errors for the measurement of Br($Z \rightarrow J + X$).

Production Mechanism		Meas. A	Meas. B
singlet quark fragmentation	ϵ_{p}^1 (%)	33.2	35.6
singlet gluon fragmentation	ϵ_{p}^1 (%)	19.5	21.1
singlet gluon radiation	ϵ_{p}^1 (%)	28.7	28.0
octet gluon fragmentation	ϵ_{p}^1 (%)	25.6	27.5
average	ϵ_{p}^1 (%)	26.9	28.9
B decay	ϵ_{b}^1 (%)	27.7	26.2

Table 3: General selection (1) efficiencies for J mesons for measurements A and B, respectively. The quantity ϵ_{p}^1 corresponds to the efficiency for selecting prompt J mesons and ϵ_{b}^1 is the efficiency for selecting J mesons originating from b-hadron decays, respectively. The channels $J \rightarrow \mu^+\mu^-$ and $J \rightarrow e^+e^-$ are combined.

Production Mechanism		Meas. A	Meas. B
singlet quark fragmentation	ϵ_p^2 (%)	8.9	4.8
singlet gluon fragmentation	ϵ_p^2 (%)	6.5	3.8
singlet gluon radiation	ϵ_p^2 (%)	16.2	11.0
octet gluon fragmentation	ϵ_p^2 (%)	20.6	15.2
average	ϵ_p^2 (%)	16.7	11.8
B decay	ϵ_b^2 (%)	0.3	0.35

Table 4: Selection (2) efficiencies for prompt J mesons of measurements A and B, respectively. The quantity ϵ_p^2 corresponds to the efficiency for selecting prompt J mesons, and ϵ_b^2 is the efficiency for selecting J mesons originating from b-hadron decays, respectively. The channels $J \rightarrow \mu^+\mu^-$ and $J \rightarrow e^+e^-$ are combined.

Error Source	$(\Delta f_p / f_p)$ (%)	
	Meas. A	Meas. B
fitting / background counting	± 16	± 5
MC E_J / E_{30} modelling	± 6	—
MC $\alpha_{J\text{-jet}}$ modelling	—	± 8
MC efficiency correction	± 8	± 8
MC statistics	± 2	± 2
Total	± 20	± 13

Table 5: Sources and magnitudes of systematic errors for the measurements A and B of f_p .

Υ Source	$\epsilon_{\Upsilon \rightarrow \mu^+\mu^-}$ (%)	$\epsilon_{\Upsilon \rightarrow e^+e^-}$ (%)	UL on $\text{Br}(Z \rightarrow \Upsilon(1S) + X)$
singlet quark fragmentation	28.5	34.3	4.19×10^{-5}
singlet gluon fragmentation	19.6	22.6	5.59×10^{-5}
singlet gluon radiation	27.8	29.1	4.54×10^{-5}
octet gluon fragmentation	27.3	29.8	4.52×10^{-5}
octet gluon radiation	35.4	39.5	3.57×10^{-5}
weighted sum	—	—	4.40×10^{-5}

Table 6: Υ selection efficiencies and measured upper limits (UL) on the branching ratios at the 95% CL for each of the theoretical models of Υ production.

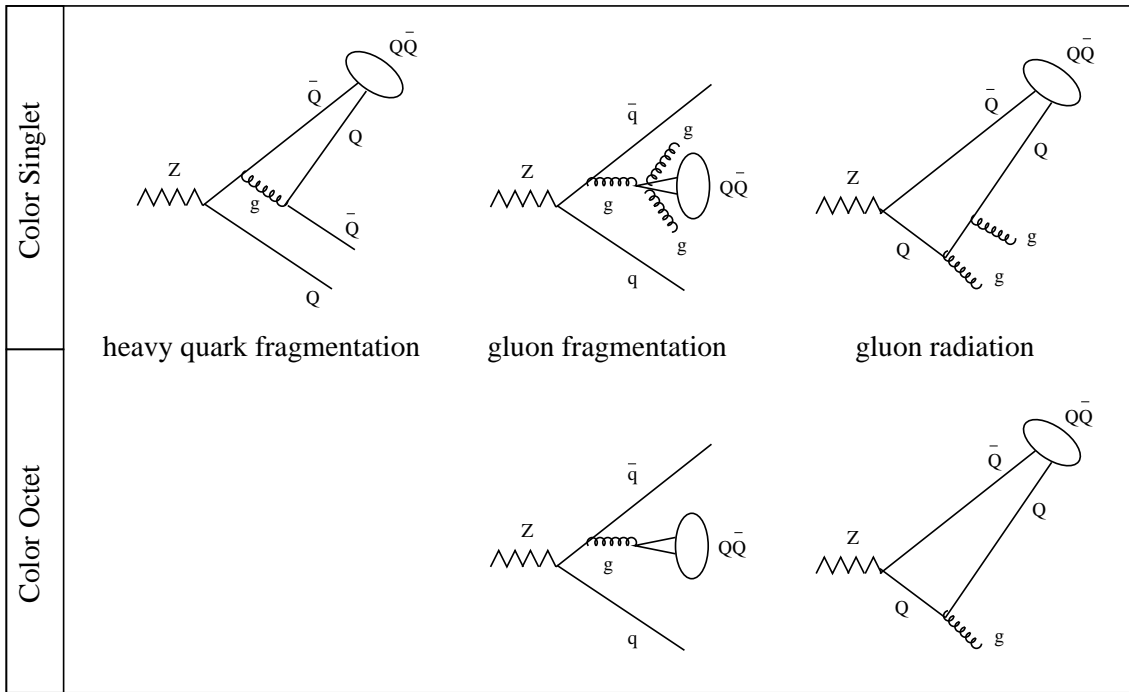


Figure 1: The colour singlet (upper row) and colour octet (lower row) Feynman diagrams illustrating the three main QCD mechanisms for heavy quarkonium production in Z decays.

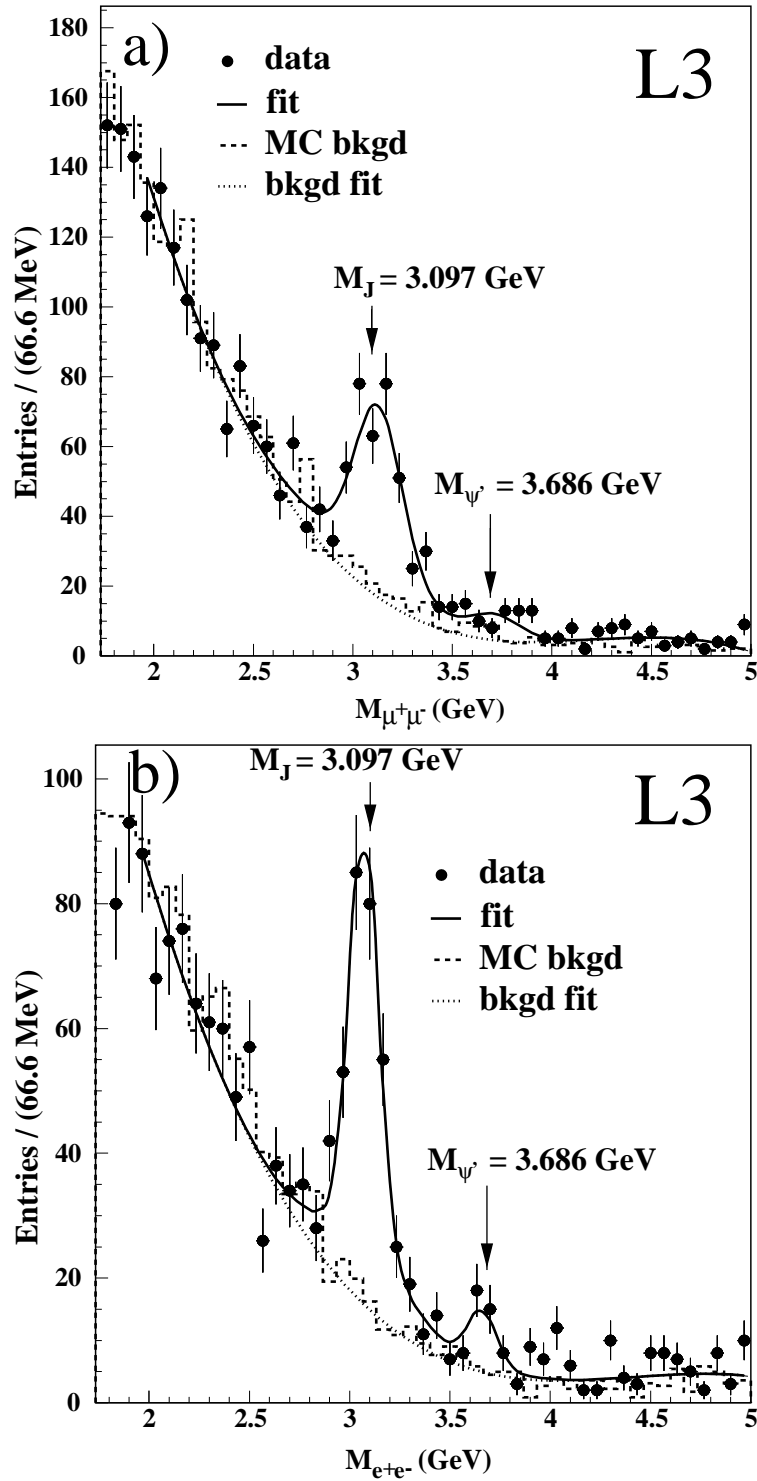


Figure 2: The invariant mass distributions for a) $\mu^+\mu^-$ and b) e^+e^- . The points are the data and the histogram is the Monte Carlo background prediction. The solid line is the fit to the data and the dashed line is the fit to the background.

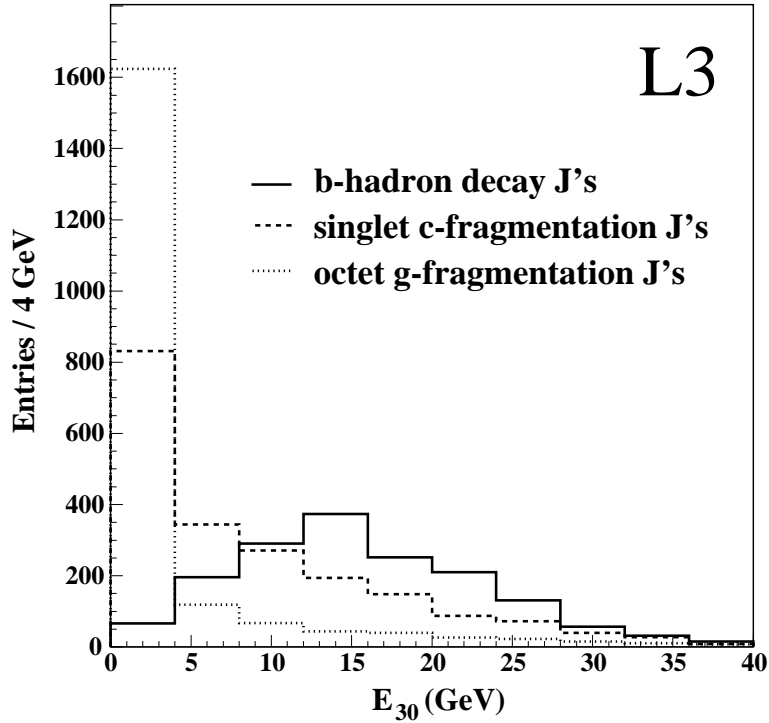


Figure 3: The Monte Carlo distributions of the energy in a 30° cone around the J direction (excluding the J energy), E_{30} , for different J sources.

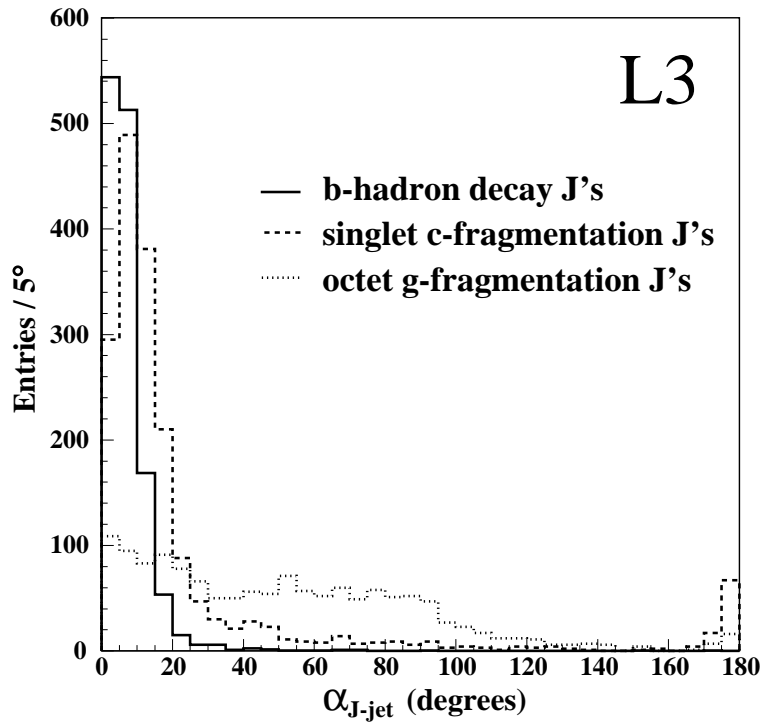


Figure 4: The Monte Carlo distributions of the angle between the J and the nearest jet (with the J leptons subtracted), $\alpha_{J\text{-jet}}$, for different J sources.

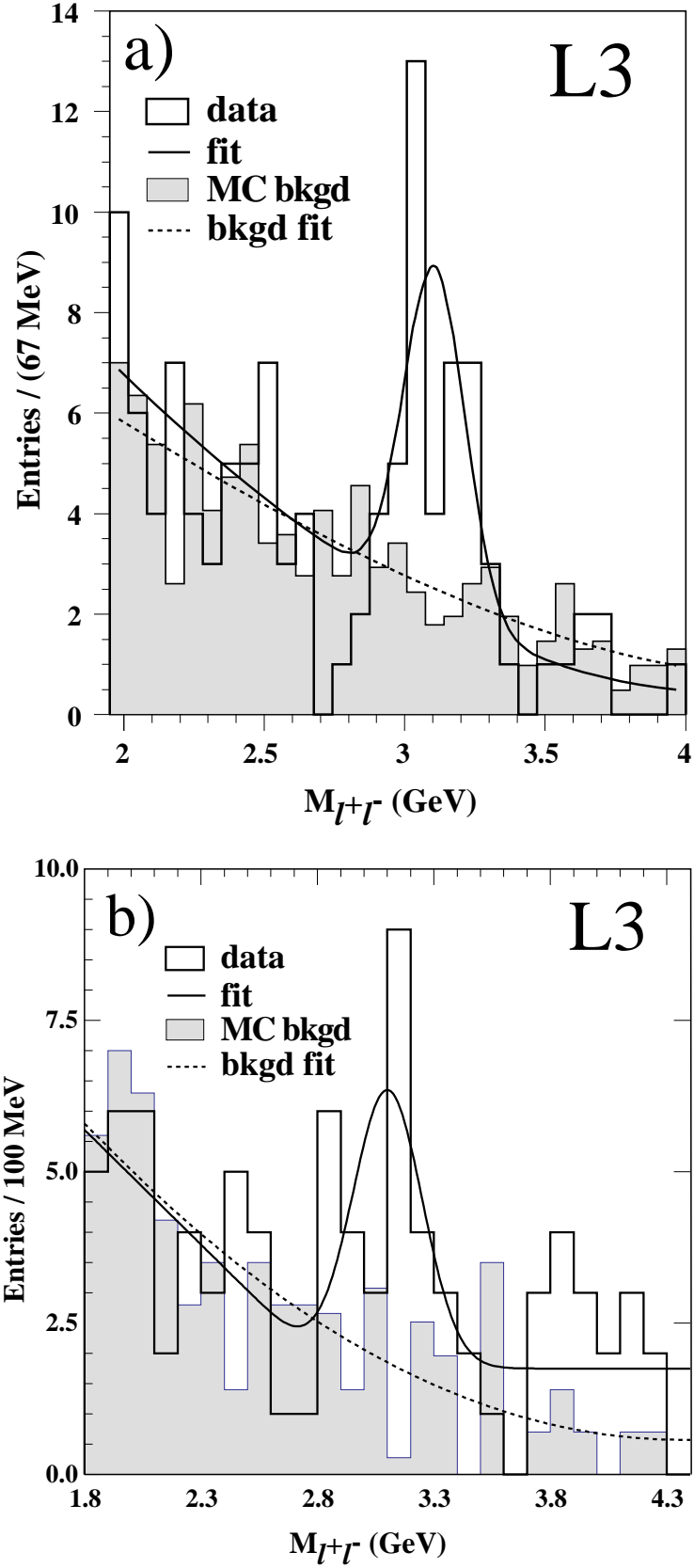


Figure 5: The prompt J selection invariant mass distributions for a) measurement A and b) measurement B ($\mu^+\mu^-$ and e^+e^- channels combined). The histogram is the data and the shaded area is the Monte Carlo background prediction.

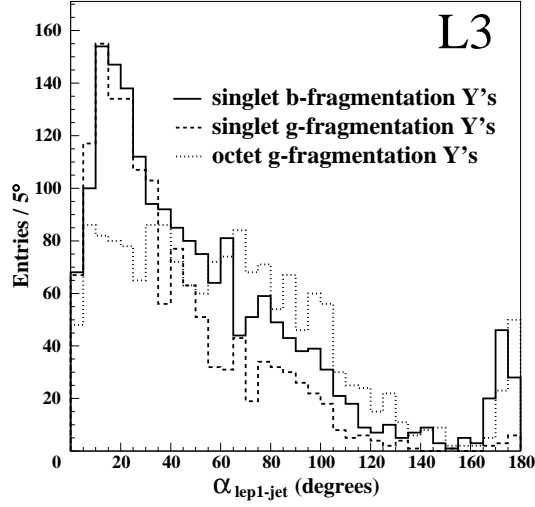


Figure 6: The Monte Carlo distributions of the angle between the most energetic lepton in the Υ candidate and the nearest jet (with the Υ leptons subtracted) for different Υ sources.

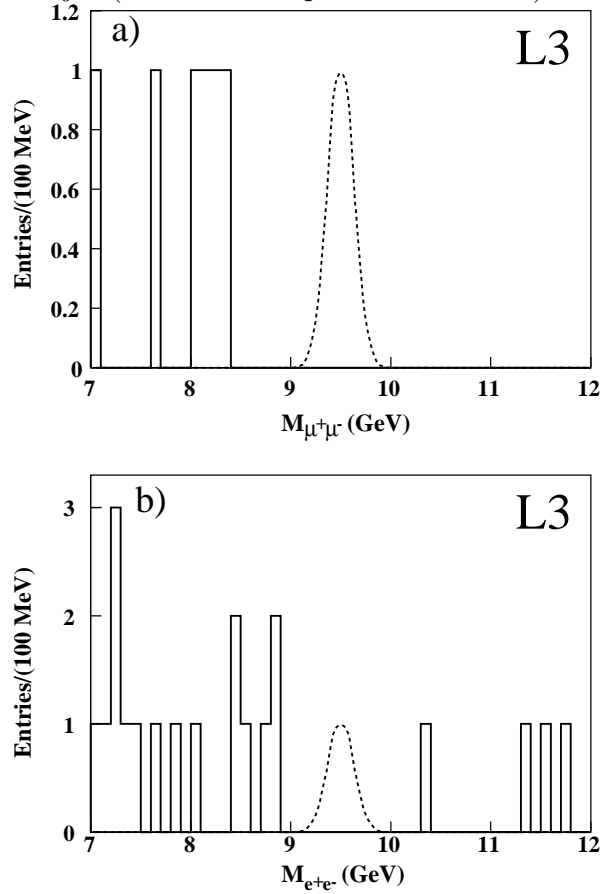


Figure 7: The Υ invariant mass distributions for the a) $\mu^+\mu^-$ and b) e^+e^- channels. The dashed lines indicate the position of the $\Upsilon(1S)$.